



Research article

The migration of metastatic breast cancer cells is regulated by matrix stiffness via YAP signalling

Wei Chen^a, Shihyun Park^b, Chishma Patel^b, Yuxin Bai^b, Karim Henary^a, Arjun Raha^a, Saeed Mohammadi^d, Lidan You^c, Fei Geng^{a,d,*}^a Department of Mechanical Engineering, McMaster University, Hamilton, ON L8S 0A3, Canada^b Faculty of Health Sciences, McMaster University, Hamilton, ON L8S 4K1, Canada^c Department of Mechanical & Industrial Engineering, University of Toronto, Toronto, ON M5S 3G8, Canada^d W Booth School of Engineering Practice and Technology, McMaster University, Hamilton, ON L8S 0A3, Canada

ARTICLE INFO

Keywords:

Cell mobility
Matrix stiffness
Mechanosensing
Metastatic breast cancer
YAP

ABSTRACT

Matrix stiffness is a driver of breast cancer progression and mechanosensitive transcriptional activator YAP plays an important role in this process. However, the interplay between breast cancer and matrix stiffness, and the significance of this interplay remained largely unknown. Here, we showed an increase in YAP nuclear localization and a higher proliferation rate in both highly metastatic MDA-MB-231 cells and the non-metastatic counterpart MCF-7 cells when they were exposed to the stiff matrix. However, in response to the stiff matrix highly metastatic MDA-MB-231 cells instead of MCF-7 cells exhibited upregulated mobility, which was shown to be YAP-dependent. Consistently, MDA-MB-231 cells exhibited different focal adhesion dynamics from MCF-7 cells in response to matrix stiffness. These results suggested a YAP-dependent mechanism through which matrix stiffness regulates the migratory potential of metastatic breast cancer cells.

1. Introduction

Extracellular matrix (ECM) stiffness is considered to be one of the most influential risk factors for cancer progression (Lee et al., 2019; Martin and Boyd, 2008; McConnell et al., 2016) and regulates cancer malignancy (Provenzano et al., 2008).

As the hallmark of cancer malignancy, metastasis is a multistep process that includes cell migration (Tahtamouni et al., 2019; Ritch et al., 2019), which required numerous mechanisms led by cytoskeleton dynamics and Focal adhesion (FA) alterations (Ritch et al., 2019). FA dynamics is a continuous process involving coordination between FA and actin cytoskeleton and is shown to be essential for cell migration (Hu et al., 2014). As a main component of FA (Crawford et al., 2003), paxillin is essential for cell migration and acts as a molecular adapter aiding in implementing changes in the organization of actin cytoskeleton (Deramandt et al., 2014).

Breast cancer metastasis of a variety of vital organs, such as bone, is one of the leading causes of breast cancer mortality (Lu and Kang, 2007). However, breast cancer metastasis is regarded as a highly inefficient process due to the fact that less than 0.01% of circulating tumour cells

eventually succeed in forming secondary tumours (Langley and Fidler, 2011). Some breast cancer cells remain dormant while other cells become more metastatic (Barkan et al., 2010). The fate of the metastatic process is determined by a complex series of interactions between breast cancer cells and metastatic sites (Langley and Fidler, 2011), and thus, it would be critical to understand the mechanisms involved in this complex dialogue.

The development of circulating breast cancer cells on the metastatic sites has been attributed to mechanical factors such as matrix stiffness (Braun et al., 2005). Among the metastatic sites for breast cancer, the stiffness of cellular matrix varies considerably (Ondeck et al., 2019). As a mechanosensitive transcriptional regulator with a significant role in cancer, Yes-associated protein (YAP) set responsiveness to the substrate stiffness (Aragona et al., 2013a). The subcellular localization of YAP is in either the cytoplasm or the nucleus, and the latter allows YAP binding and activation of transcriptional enhanced associate domain (TEAD) (Dupont et al., 2011). As the target gene of YAP, connective tissue growth factor (CTGF) enhances the motility of breast cancer cells (Chen et al., 2007). Through the modulation of YAP signalling, ECM stiffness induces the phenotypic changes of breast cancer, including cell proliferation and

* Corresponding author.

E-mail address: gengf@mcmaster.ca (F. Geng).

migration (Haga et al., 2005; Ishihara et al., 2013; Paszek et al., 2005; Umesh et al., 2014). The mechanical cues are transduced intracellularly through YAP, which then enhances cancer metastasis (Zanconato et al., 2016). However, the role of YAP mechanosensing in the complex interplay between breast cancer and matrix remained unclear (Barkan et al., 2010; Guise, 2010; Langley and Fidler, 2007).

Previously we have demonstrated metastatic breast cancer promotes the accumulation of YAP in the nucleus, thus giving the cells metastatic advantage (Chen et al., 2019a). In this paper, we demonstrated that migration of metastatic breast cancer cells is promoted by stiff matrix in a YAP-dependent manner.

2. Materials and methods

2.1. Preparation of PDMS substrates for cell culture

Polydimethylsiloxane (PDMS) (Sylgard® 184, Dow Corning) base and crosslinker were mixed at three different ratios (by weight) of 1:5, 1:10, and 1:20 as described previously (Park et al., 2010). Mixtures were poured onto prepared 24-well plates (Thermo Fisher Scientific), cured at room temperature overnight (Figure 1). Resistance to deformation is defined by the Young's elastic modulus, E , obtained by applying a tensile force (stress) to a sample with a defined cross-sectional area and measuring the relative change in length (strain). PDMS stiffness was measured by microindentation using a Biomomentum Mach-1 system (Biomomentum Inc) as described previously (Ireland et al., 2020). The base reagent is known to contain 0.5% xylene, 0.2% ethylbenzene, 60% dimethylvinyl-terminated dimethyl siloxane, 30–60% dimethylvinylated and trimethylated silica and 1–5% tetra (trimethylsiloxy) silane.

Crosslinking agent contains 0.19% xylene, 0.1% ethylbenzene, 55–75% dimethyl, methylhydrogen siloxane, 15–35% dimethylvinyl-terminated dimethyl siloxane, 10–30% dimethylvinylated and trimethylated silica and 1–5% tetramethyl tetra vinyl cyclotetrasiloxane. The standard ratio for PDMS preparation is 1:10 as per the instruction of PDMS supplier Dow Corning. 1:5 and 1:20 ratios were chosen to extend PDMS stiffness range in order to identify the responses of breast cancer to matrix stiffness.

2.2. Cell culture and reagents

Human breast epithelial cell line MCF-10A cells and human breast cancer cell line MCF-7 cells were purchased from American Type Culture Collection (ATCC). MDA-MB-231 and Hs 578T cells were kindly provided by Dr. Juliet Daniel at McMaster University. MCF-7 and MDA-MB-231 cells were cultured in Dulbecco's Modified Eagle's Medium (DMEM, Thermo Fisher Scientific) supplemented with 10% Fetal Bovine Serum (FBS, Thermo Fisher Scientific). All cell cultures were incubated at 37 °C with 5% CO₂. Both the cell types were grown on PDMS and plastic substrates on 24 well plates (Thermo Fisher Scientific).

2.3. RNA extraction

MCF-7 and MDA-MB-231 cells were seeded and cultured on PDMS and plastic substrates. Then the cells were harvested and total RNAs were extracted using PureLink RNA Mini kit (Thermo Fisher Scientific) according to the manufacturer's directions. RNA concentrations were then measured using Qubit Fluorometer and Qubit RNA Assay Kit (Thermo Fisher Scientific).

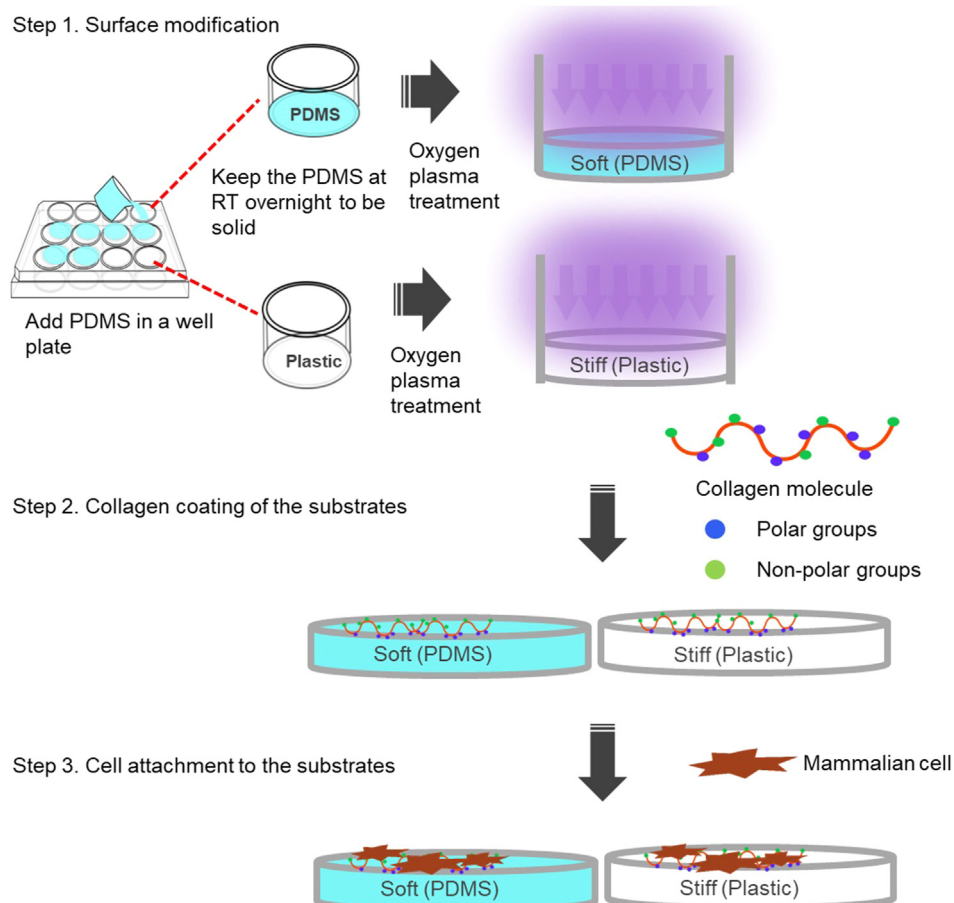


Figure 1. The preparation of PDMS and plastic substrates for mammalian cell culture. PDMS and plastic substrates on well plates were subject to plasma treatment and collagen coating prior to the mammalian cell attachment.

2.4. qRT-PCR

YAP and CTGF gene expression were analyzed using quantitative reverse transcription polymerase chain reaction (qRT-PCR) with GAPDH as the internal reference gene. SYBR Green Quantitative qRT-PCR kit was obtained from Sigma-Aldrich. YAP gene was amplified using: YAP forward primer: 5′GCACCTCTGTGTTTAAAGGGTCT-3′; YAP reverse primer: 5′-CAACTTTTGCCTCCTCAA-3′. CTGF gene was amplified using: CTGF forward primer: 5′-AGGAGTGGGTGTGTGACGA-3′; CTGF reverse primer: 5′-CCAGGCAGTTGGCTCTAATC-3′. GAPDH gene was amplified using: GAPDH forward primer: 5′-CTCCTGCACCACCAACTGCT-3′; GAPDH reverse primer: 5′-GGCCATCCACAGTCTCTG-3′. The procedures were described previously (Chen et al., 2019b).

2.5. YAP immunofluorescence staining

For the analysis of YAP nucleus localization, MCF-7 cells or MDA-MB-231 cells were fixed with 4% paraformaldehyde and permeabilized in 0.1% Triton X-100. Then, the cells were washed with PBS and blocked with 5% PBS-BSA at 4 °C overnight. Then the cells were incubated with mouse anti human YAP monoclonal antibody (Santa Cruz Biotechnology) followed by fluorescein isothiocyanate (FITC)-conjugated goat anti-mouse secondary antibody (Sigma-Aldrich). Cell nuclei of each sample were stained with 4′,6-Diamidino-2-phenylindole dihydrochloride (DAPI, Thermo Fisher Scientific) and imaged on Olympus inverted phase contrast and fluorescence microscope (IX51S1F-3, Olympus). For paxillin

immunofluorescence, mouse anti-human paxillin monoclonal antibody (Thermo Fisher Scientific) was used.

2.6. Colocalization analysis

CellProfiler (www.cellprofiler.org) was used to quantify YAP nuclear/cytoplasmic intensity in immunofluorescence images and YAP/DAPI colocalization was measured via the correlation between the intensities of green and blue channels on a pixel-by-pixel basis across an entire image. The Cell Profiler colocalization pipeline was carried out to calculate the correlation and colocalization (Manders Coefficient) between the pixel intensities.

2.7. Gap closure assay

1×10^5 MCF-7, Hs 578T and MDA-MB-231 cells were seeded on PDMS and plastic substrates on 24 well plates. Cells were grown to form a confluent monolayer in the wells before wounding. A sterilized pipette tip was used to generate wounding across the cell monolayer, and the debris was washed with PBS. At varying intervals, the cells migrating into the wounded area were visualized and photographed at 0 and 24 h under an inverted microscope (IX51S1F-3, Olympus). The distance between cell front was measured at 0 h and 24 h time-points using ImageJ. To measure the average healing speed inside the wound area at each time-point, the following equation was used as described previously (Pijuan et al., 2019).

$$v (\mu\text{m}/\text{h}) = [\text{Distance initial time } (\mu\text{m}) - \text{Distance final time } (\mu\text{m})] / \text{Total time (h)}$$

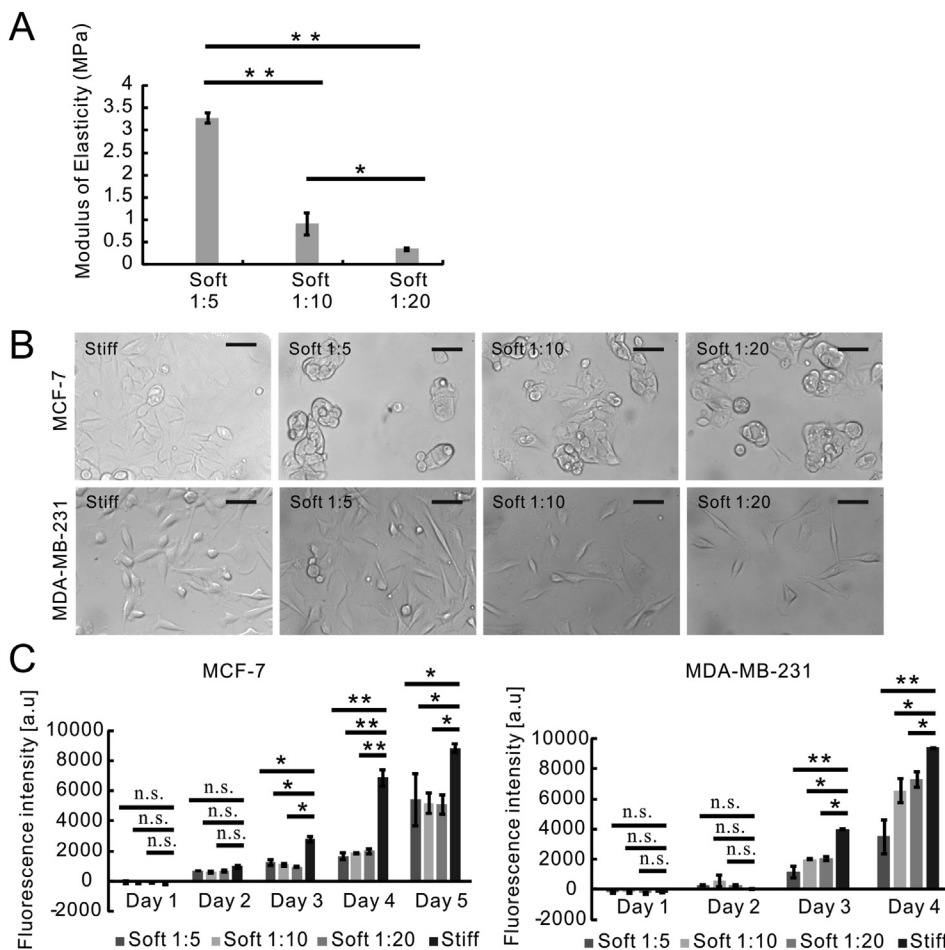


Figure 2. Stiff matrix improved proliferation rates of both metastatic and non-metastatic cancer cells. (A) The determination of modulus of elasticity of three types of PDMS substrates. Data were represented as means \pm SD (n = 5). **P < 0.01, *P < 0.05. (B) Phase contrast microscopy of MCF-7 and MDA-MB-231 cells that were cultured on plastic (Stiff) or PDMS substrates (Soft 1:5, Soft 1:10, Soft 1:20); Scale bar, 10 μm . (C) The proliferation analysis of MCF-7 and MDA-MB-231 cells that were cultured on plastic (Stiff) or PDMS substrates (Soft 1:5, Soft 1:10, Soft 1:20) using Alamar Blue assay. Data were represented as means \pm SD (n = 3). **P < 0.01, *P < 0.05, n.s. not significant.

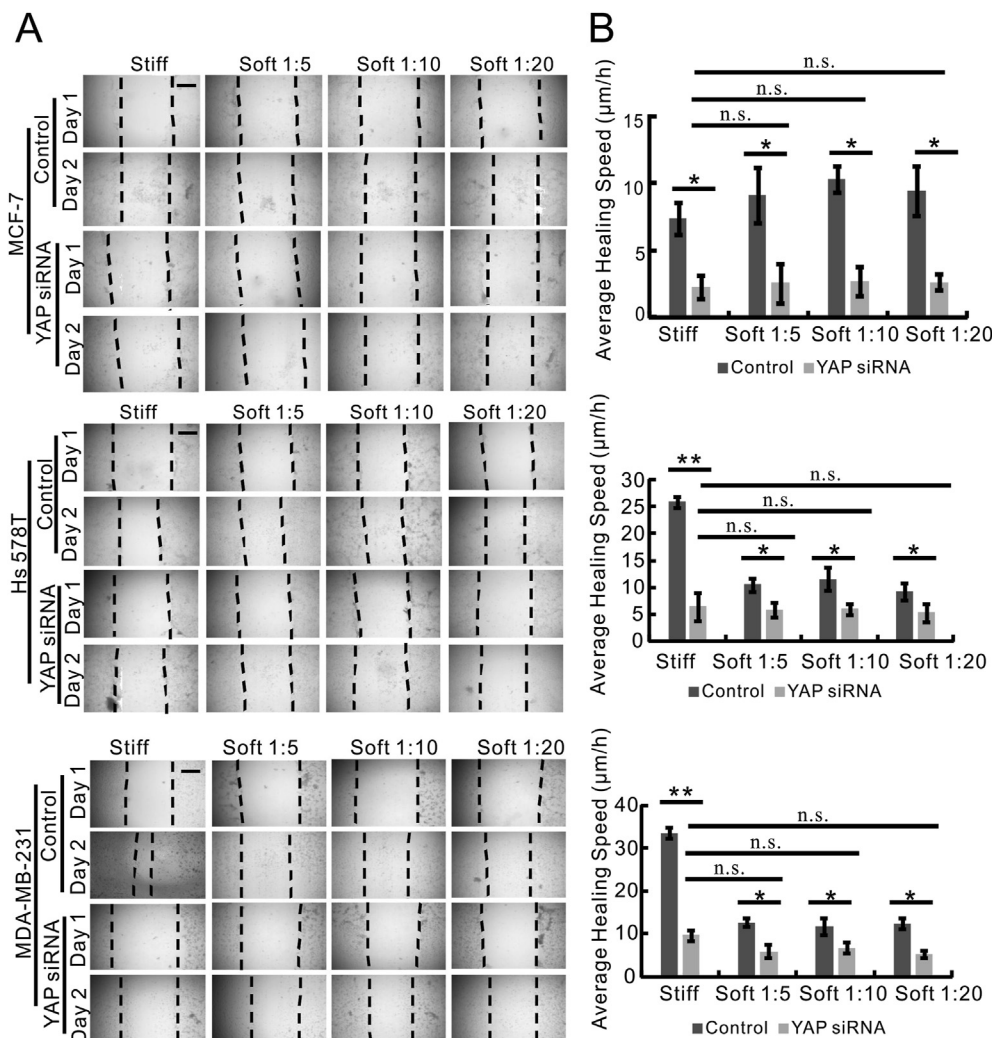


Figure 3. Migration of metastatic breast cancer cells was promoted by stiff matrix in a YAP-dependent manner. (A) Time-lapse microscopy images of gap closure of MCF-7, Hs 578T and MDA-MB-231 cells that were cultured on stiff (plastic) or soft (PDMS) substrates (Soft 1:5, Soft 1:10, Soft 1:20) at 0 h (Day 1) and 24 h (Day 2) after scratch was created. The dotted lines define the area lacking cells. Scale bar, 100 µm. (B) The quantification of Gap Closure Assay in Figure 3A using ImageJ. The average healing speed (µm/h) of MCF-7 (top graph), Hs 578T (middle graph) and MDA-MB-231 cells (bottom graph) was shown. Data were represented as means ± SD (n = 3). *P < 0.05.

2.8. YAP siRNA transfection

Pre-designed siRNAs (On-Target plus SMART pool targeting Control and YAP) were purchased from Dharmacon. For siRNA transfection experiments, MCF-7, Hs 578T and MDA-MB-231 cells were grown to form a confluent monolayer on 24 well plates, subject to the wounding, and then transfected with 100 nM of the indicated siRNA using DharmaFECT transfection reagent (Dharmacon), following the manufacturer's protocol.

2.9. Statistical analysis

The statistical analysis in this paper was reported as mean ± SD. For the evaluation of differences, unpaired 2-tailed Student's t-test was performed assuming equal variance. Differences were considered significant at P < 0.05.

3. Results

3.1. The development and stiffness measurement of soft (PDMS) substrates

Silicone elastomers such as PDMS are usually used to form elastic membranes (Mohammed et al., 2019). The intrinsic PDMS properties make it an appropriate choice of polymer for mechanobiology applications (Park et al., 2010). In this research, we examined the effects of

matrix stiffness on YAP nucleocytoplasmic shuttling, proliferation and mobility of breast cancer cells that were cultured on collagen coated soft (PDMS) substrates or stiff (plastic) substrate. The comparative analysis of plastic versus soft polymers has been performed extensively in mechanobiology research (Aragona et al., 2013b; Nukuda et al., 2015; Panciera et al., 2020).

PDMS stiffness was adjusted by varying the ratio of curing agent to base used during polymer mixing. Different mixing ratios yield different proportions of crosslinked and uncrosslinked polymers after curing, which vary the stiffness of the cured polymer (Park et al., 2010; Seghir and Arscott, 2015). Thus, we fabricated PDMS substrates using three mixing ratios (curing agent to base) of 1:5, 1:10, and 1:20 across a range of matrix stiffnesses to investigate the regulation of matrix stiffness in breast cancer metastasis. The standard ratio (curing agent to base) for PDMS preparation is 1:10 as per the instruction of supplier. 1:5 and 1:20 ratios were chosen to extend PDMS stiffness range in order to identify the responses of breast cancer to matrix stiffness as described previously (Dupont et al., 2011; Park et al., 2010; Sotiri et al., 2018). PDMS and plastic substrates were subject to oxygen plasma treatment and collagen coating prior to the mammalian cell attachment (Figure 1). The modulus of elasticity measurements showed that tensile strength of PDMS substrates correlated linearly to the proportion of crosslinker, and the Young's modulus was determined to be 3.28 MPa for the PDMS of 1:5 mixing ratio, 0.92 MPa for the PDMS of 1:10 mixing ratio, and 0.35 MPa for the PDMS of 1:20 mixing ratio (Figure 2A). As a comparison to soft PDMS substrates, the plastic substrate (tissue culture polystyrene) has a Young's modulus of 1 GPa (GPa) (Syed et al., 2015).

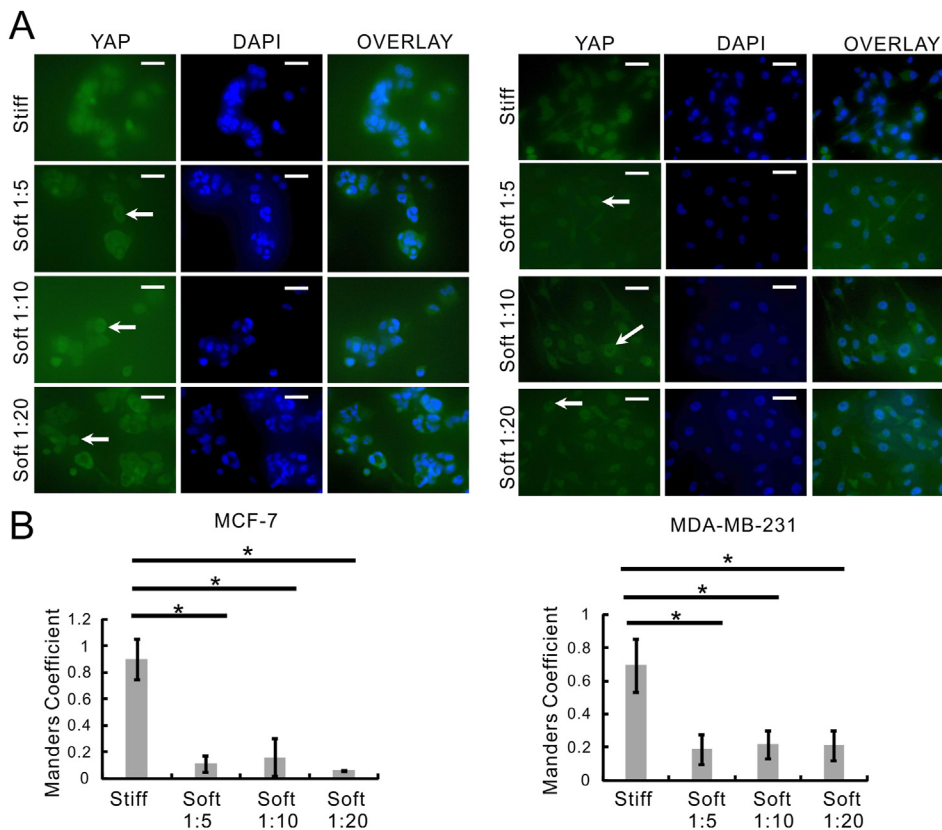


Figure 4. Both metastatic and non-metastatic cancer cell lines exhibited increased YAP nuclear entry in response to stiff matrix. (A) MCF-7 and MDA-MB-231 cells were cultured on stiff (plastic) or soft (PDMS) substrates (Soft 1:5, Soft 1:10, Soft 1:20) and then YAP subcellular localization in those cells was analyzed by immunofluorescence staining. The cells showing nuclear exclusion of YAP were highlighted by arrowheads. Field-of-views were selected randomly under each condition and photographed at a magnification of 40 ×. Scale bar, 10 μm; (B) Colocalization analysis of YAP and DAPI in the cells from Figure 4A were analyzed using CellProfiler. Data were represented as means ± SD (n = 3). *P < 0.05.

3.2. Matrix stiffness altered the morphology of non-metastatic breast cancer cells instead of metastatic breast cancer cells

As shown in Figure 1, we performed the surface modification on stiff (plastic) and soft (PDMS) substrates by oxygen plasma treatment and collagen coating (Figure 1). To investigate the effects of matrix stiffness on breast cancer behaviours, we used highly metastatic breast cancer cell line (MDA-MB-231) and non-metastatic counterpart cell line (MCF-7) (Liu et al., 2019). Phase contrast microscopy demonstrated that MDA-MB-231 cells exhibited the spindle-shaped morphologies both on stiff (plastic) and soft (PDMS) substrates (Figure 2B). MCF-7 cells on stiff substrate were flat with cobblestone-like morphology (Figure 2B). By comparison, MCF-7 cells on soft (PDMS) substrates acquired spherical morphology and formed aggregates (Figure 2B).

3.3. Both metastatic and non-metastatic cancer cells gained higher proliferation rates in response to stiff matrix

The metastatic potentials of MCF-7 and MDA-MB-231 cells were characterized in our previous studies (Chen et al., 2019b), and their proliferation rates on different substrates were compared using Alamar Blue assay in Figure 2C. The results showed that MDA-MB-231 cells acquired a significantly higher growth rate on the plastic substrate compared with all PDMS substrates (Figure 2C). However, both MCF-7 and MDA-MB-231 cells maintained a similar proliferation rate among the three types of PDMS substrates (Figure 2C).

3.4. Migration of metastatic breast cancer cells was promoted by stiff matrix in a YAP-dependent manner

Then we sought to understand the effects of matrix stiffness on the migratory capacity of breast cancer cells with distinct metastatic potential. Thus, we employed the gap closure assay to assess the mobility of highly metastatic MDA-MB-231 and Hs 578T cells in comparison to non-

metastatic MCF-7 cells when they were grown on stiff and soft substrates. The images of the gap closure assay were shown in Figure 3A and quantified in Figure 3B. MCF-7 cells that were cultured on soft (PDMS) and stiff (plastic) substrates exhibited a similar rate of gap closure, which was reflected by the average healing speed (Figure 3B). In comparison, Hs 578T and MDA-MB-231 cells on the stiff (plastic) substrate displayed a higher average healing speed than the cells grown on the soft (PDMS) substrates (Figure 3B). However, there was no significant difference in the average healing speed of cells between stiff and soft substrates when MCF-7, Hs 578T and MDA-MB-231 cells were transfected with siRNA targeting against YAP (Figure 3B).

3.5. Increased YAP nuclear entry was shown in both metastatic and non-metastatic cancer cells on stiff matrix

To better understand the effects of matrix stiffness on YAP nucleo-cytoplasmic shuttling, we performed the YAP intracellular localization analysis in MCF-7 and MDA-MB-231 cells cultivated on soft (PDMS) and stiff (plastic) substrates. Then we conducted fluorescent microscopy of YAP (Figure 4A, green channel) and DAPI (Figure 4A, blue channel) and colocalization analysis of the two channels (Figure 4B) to measure YAP nucleo-cytoplasmic shuttling.

YAP was shown to locate mostly outside the nucleus (Figure 4A, arrow heads) in both MCF-7 and MDA-MB-231 cells that were grown on soft (PDMS) substrates. When both the cell lines were cultured on stiff (plastic) substrate, YAP was evenly distributed intracellularly (Figure 4A). Consistently, higher colocalization between YAP and DAPI (YAP nuclear entry) was observed in MCF-7 cells and MDA-MB-231 cells that were cultured on stiff (plastic) substrate (Manders Coefficient 0.9 and 0.7 respectively) (Figure 4B). Whereas MCF-7 cells and MDA-MB-231 cells grown on soft (PDMS) substrates displayed significantly less YAP and DAPI colocalization (Manders Coefficient close to or less than 0.2).

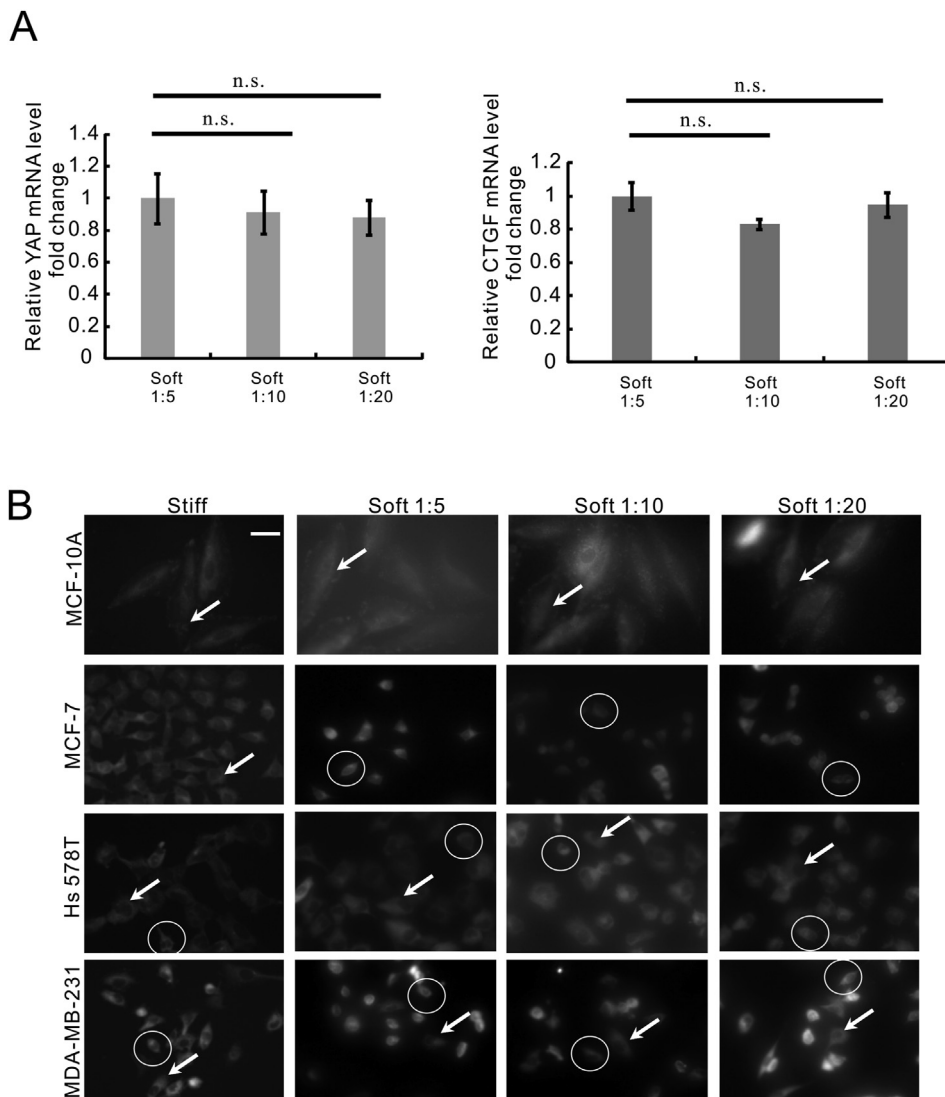


Figure 5. Focal adhesion dynamics in metastatic breast cancer cells were regulated by matrix stiffness. (A) qRT-PCR analysis of YAP (left panel) and CTGF (right panel) gene expression in MCF-7 and MDA-MB-231 cells that are cultured on stiff (plastic) or soft (PDMS) substrates (Soft 1:5, Soft 1:10, Soft 1:20). Data were represented as means \pm SD (n = 3). n.s. not significant. (B) The paxillin staining in MCF-10A, MCF-7, Hs 578T and MDA-MB-231 cells that were cultured on stiff (plastic) or soft (PDMS) substrates (Soft 1:5, Soft 1:10, Soft 1:20). Field-of-views were selected randomly under each condition and photographed at a magnification of 40 \times . Scale bar, 10 μ m. The representative cells with diffuse staining pattern of paxillin were highlighted using arrowheads and the representative cells with perinuclear staining pattern of paxillin were highlighted using circles.

3.6. The stiffness difference between PDMS substrates did not affect YAP mRNA expression in metastatic cancer cells

As YAP nucleo-cytoplasmic shuttling was regulated by matrix stiffness (Figure 4), we sought to identify whether YAP gene expression in MDA-MB-231 cells sensed the stiffness differences between the three PDMS substrates. Due to the low expression of YAP signalling in MCF-7 cells, we conducted the mRNA analysis in MDA-MB-231 cells that were cultivated on PDMS using qRT-PCR analysis. The results showed no difference in the gene expression of YAP (Figure 5A, left) and its target gene CTGF (Figure 5A, right) in MDA-MB-231 cells cultivated on the three types of PDMS substrates. The results indicated that YAP-dependent mechanotransduction might not differentiate the range (0.35 MPa–3.28 MPa) of matrix stiffness.

3.7. Focal adhesion dynamics in metastatic breast cancer cells were regulated by matrix stiffness

Figure 3 showed that MDA-MB-231 and Hs 578T cells acquired higher migratory potential on the stiff (plastic) substrate. In order to characterize the FAs dynamics associated with mobility increase of metastatic breast cancer cells, we performed paxillin staining with MCF-10A, MCF-7, Hs 578T, and MDA-MB-231 cells that were cultured on the substrates with different amount of stiffness. A similar diffuse cytoplasmic staining

pattern of paxillin was observed in non-cancerous MCF-10A cells cultured on the stiff (plastic) and soft (PDMS) substrates (Figure 5B, highlighted by arrowheads). Metastatic breast cancer cell lines MDA-MB-231 and Hs 578T cells exhibited a mix of both diffuse cytoplasmic staining pattern (Figure 5B, highlighted by arrowheads) and perinuclear staining pattern (Figure 5B, highlighted by circles) when cultured on the stiff (plastic) and soft (PDMS) substrates. Whereas most of MCF-7 cells on the soft substrate (PDMS) displayed perinuclear staining pattern of paxillin (Figure 5B, highlighted by circles) in comparison to the cells on stiff substrate (plastic).

4. Discussion

ECM stiffness of metastatic sites (bone, lung, brain and lymph node) is linked to biochemical signalling in breast cancer, which influences the outcome of cancer metastasis (Ulbricht et al., 2013). Although YAP was shown to be the central hub regulating cancer proliferation and metastasis, the significance of YAP orchestrated mechanotransduction in the outcome of breast cancer metastasis remains unclear (Lamar et al., 2012; Ondeck et al., 2019; Wu and Yang, 2018). In this paper, we identified a YAP-dependent cellular mechanism through which metastatic breast cancer cells enhance their migratory potential on stiff matrix.

YAP is primarily controlled at the level of the nucleocytoplasmic shuttling (Shreberk-Shaked and Oren, 2019). However, the controlling

mechanisms over YAP nucleocytoplasmic shuttling orchestrates cancer behaviours are unclear (Dobrokhotov et al., 2018; Elosegui-Artola et al., 2017; Shreberk-Shaked and Oren, 2019). Most of these mechanical inputs converge on two distinct, yet interdependent signal transduction systems: the Hippo pathway and the state of the actomyosin cytoskeleton (Kofler et al., 2018). Our research characterized the effects of matrix stiffness on breast cancer metastasis via a series of cellular events such as YAP nucleocytoplasmic shuttling (Figure 4), alteration of FA dynamics (Figure 5), cell mobility enhancement (Figure 3).

This study provided the findings for the understanding of cancer behaviours that are developed in response to matrix stiffness. Firstly, the results showed that migration of metastatic breast cancer cells is regulated by matrix stiffness. And this regulation was not observed in non-metastatic breast cancer cells. Secondly, the results suggested that YAP signalling is required for the regulation of breast cancer cell migration by matrix stiffness.

5. Conclusions

To summarize, our study demonstrated that migration of metastatic breast cancer cells is promoted by stiff matrix via YAP signalling. Since initiating cell growth and migration is the most challenging step for disseminating breast cancer cells (Langley and Fidler, 2011), the continued investigation into the regulation of cancer cell migration by matrix stiffness will shed light on the mechanism of breast cancer metastasis.

Declarations

Author contribution statement

W. Chen: Conceived and designed the experiments; Performed the experiments; Analyzed and interpreted the data; Wrote the paper.

S. Park, C. Patel, Y. Bai: Contributed reagents, materials, analysis tools or data; Performed the experiments.

K. Henary: Performed the experiments.

A. Raha, S. Mohammadi: Analyzed and interpreted the data.

L. You, F. Geng: Conceived and designed the experiments; Wrote the paper.

Funding statement

This work was supported by Mitacs Accelerate Program (IT15842).

Data availability statement

Data will be made available on request.

Declaration of interests statement

The authors declare no conflict of interest.

Additional information

No additional information is available for this paper.

Acknowledgements

We are grateful to Dr. Juliet Daniel for providing human breast cancer Hs 578T and MDA-MB-231 cells.

References

Aragona, M., Panciera, T., Manfrin, A., Giullitti, S., Michielin, F., Elvassore, N., Dupont, S., Piccolo, S., 2013a. A mechanical checkpoint controls multicellular growth through YAP/TAZ regulation by actin-processing factors. *Cell* 154, 1047–1059.

Aragona, M., Panciera, T., Manfrin, A., Giullitti, S., Michielin, F., Elvassore, N., Dupont, S., Piccolo, S., 2013b. A mechanical checkpoint controls multicellular growth through YAP/TAZ regulation by actin-processing factors. *Cell* 154, 1047–1059.

Barkan, D., Green, J.E., Chambers, A.F., 2010. Extracellular matrix: a gatekeeper in the transition from dormancy to metastatic growth. *Eur. J. Cancer* 46, 1181–1188.

Braun, S., Vogl, F.D., Naume, B., Janni, W., Osborne, M.P., Coombes, R.C., Schlimok, G., Diel, L.J., Gerber, B., Gebauer, G., et al., 2005. A pooled analysis of bone marrow micrometastasis in breast cancer. *N. Engl. J. Med.* 353, 793–802.

Chen, P.S., Wang, M.Y., Wu, S.N., Su, J.L., Hong, C.C., Chuang, S.E., Chen, M.W., Hua, K.T., Wu, Y.L., Cha, S.T., et al., 2007. CTGF enhances the motility of breast cancer cells via an integrin- α 3-ERK1/2-dependent S100A4-upregulated pathway. *J. Cell Sci.* 120, 2053–2065.

Chen, W., Bai, Y., Patel, C., Geng, F., 2019a. Autophagy promotes triple negative breast cancer metastasis via YAP nuclear localization. *Biochem. Biophys. Res. Commun.* 520, 263–268.

Chen, W., Bai, Y., Patel, C., Geng, F., 2019b. Autophagy promotes triple negative breast cancer metastasis via YAP nuclear localization. *Biochem. Biophys. Res. Commun.*

Crawford, B.D., Henry, C.A., Clason, T.A., Becker, A.L., Hille, M.B., 2003. Activity and distribution of paxillin, focal adhesion kinase, and cadherin indicate cooperative roles during zebrafish morphogenesis. *Mol. Biol. Cell* 14, 3065–3081.

Deramaut, T.B., Dujardin, D., Noulet, F., Martin, S., Vauchelles, R., Takeda, K., Rondé, P., 2014. Altering FAK-paxillin interactions reduces adhesion, migration and invasion processes. *PLoS One* 9, e92059.

Dobrokhotov, O., Samsonov, M., Sokabe, M., Hirata, H., 2018. Mechanoregulation and pathology of YAP/TAZ via Hippo and non-Hippo mechanisms. *Clin. Transl. Med.* 7.

Dupont, S., Morsut, L., Aragona, M., Enzo, E., Giullitti, S., Cordenonsi, M., Zanconato, F., Le Digabel, J., Forcato, M., Bicciato, S., et al., 2011. Role of YAP/TAZ in mechanotransduction. *Nature* 474, 179–184.

Elosegui-Artola, A., Andreu, I., Beedle, A.E.M., Lezamiz, A., Uroz, M., Kosmalska, A.J., Oriá, R., Kechagia, J.Z., Rico-Lastres, P., Le Roux, A.L., et al., 2017. Force triggers YAP nuclear entry by regulating transport across nuclear pores. *Cell* 171, 1397–1410 e14.

Guise, T., 2010. Examining the metastatic niche: targeting the microenvironment. *Semin. Oncol.* 37 (Suppl 2).

Haga, H., Irahara, C., Kobayashi, R., Nakagaki, T., Kawabata, K., 2005. Collective movement of epithelial cells on a collagen gel substrate. *Biophys. J.* 88, 2250–2256.

Hu, Y.L., Lu, S., Szeto, K.W., Sun, J., Wang, Y., Lasheras, J.C., Chien, S., 2014. FAK and paxillin dynamics at focal adhesions in the protrusions of migrating cells. *Sci. Rep.* 4, 1–7.

Ireland, R.G., Kibschull, M., Audet, J., Ezzo, M., Hinz, B., Lye, S.J., Simmons, C.A., 2020. Combinatorial extracellular matrix microarray identifies novel bioengineered substrates for xeno-free culture of human pluripotent stem cells. *Biomaterials* 248, 120017.

Ishihara, S., Yasuda, M., Harada, I., Mizutani, T., Kawabata, K., Haga, H., 2013. Substrate stiffness regulates temporary NF- κ B activation via actomyosin contractions. *Exp. Cell Res.* 319, 2916–2927.

Kofler, M., Speight, P., Little, D., Di Ciano-Oliveira, C., Szász, K., Kapus, A., 2018. Mediated nuclear import and export of TAZ and the underlying molecular requirements. *Nat. Commun.* 9.

Lamar, J.M., Stern, P., Liu, H., Schindler, J.W., Jiang, Z.-G., Hynes, R.O., 2012. The Hippo pathway target, YAP, promotes metastasis through its TEAD-interaction domain. *Proc. Natl. Acad. Sci. U. S. A.* 109, E2441–E2450.

Langley, R.R., Fidler, I.J., 2007. Tumor cell-organ microenvironment interactions in the pathogenesis of cancer metastasis. *Endocr. Rev.* 28, 297–321.

Langley, R.R., Fidler, I.J., 2011. The seed and soil hypothesis revisited-The role of tumor-stroma interactions in metastasis to different organs. *Int. J. Cancer* 128, 2527–2535.

Lee, J.Y., Chang, J.K., Dominguez, A.A., Lee, H., pyo, Nam, S., Chang, J., Varma, S., Qi, L.S., West, R.B., Chaudhuri, O., 2019. YAP-independent mechanotransduction drives breast cancer progression. *Nat. Commun.* 10, 1–9.

Liu, Y.L., Chou, C.K., Kim, M., Vasisht, R., Kuo, Y.A., Ang, P., Liu, C., Perillo, E.P., Chen, Y.A., Blocher, K., et al., 2019. Assessing metastatic potential of breast cancer cells based on EGFR dynamics. *Sci. Rep.* 9.

Lu, X., Kang, Y., 2007. Organotropism of breast cancer metastasis. *J. Mammary Gland Biol. Neoplasia* 12, 153–162.

Martin, L.J., Boyd, N.F., 2008. Mammographic density: Potential mechanisms of breast cancer risk associated with mammographic density: hypotheses based on epidemiological evidence. *Breast Cancer Res.* 10, 1–14.

McConnell, J.C., O'Connell, O.V., Brennan, K., Weiping, L., Howe, M., Joseph, L., Knight, D., O'Cuallain, R., Lim, Y., Leek, A., et al., 2016. Increased peri-ductal collagen micro-organization may contribute to raised mammographic density. *Breast Cancer Res.* 18, 1–17.

Mohammed, D., Versaavel, M., Bruyère, C., Alaimo, L., Luciano, M., Vercruyse, E., Procès, A., Gabriele, S., 2019. Innovative tools for mechanobiology: unraveling outside-in and inside-out mechanotransduction. *Front. Bioeng. Biotechnol.* 7.

Nukuda, A., Sasaki, C., Ishihara, S., Mizutani, T., Nakamura, K., Ayabe, T., Kawabata, K., Haga, H., 2015. Stiff substrates increase YAP-signaling-mediated matrix metalloproteinase-7 expression. *Oncogenesis* 4 e165–e165.

Ondek, M.G., Kumar, A., Placone, J.K., Plunkett, C.M., Matte, B.F., Wong, K.C., Fattet, L., Yang, J., Engler, A.J., 2019. Dynamically stiffened matrix promotes malignant transformation of mammary epithelial cells via collective mechanical signaling. *Proc. Natl. Acad. Sci. U. S. A.* 116, 3502–3507.

Panciera, T., Citron, A., Di Biagio, D., Battilana, G., Gandin, A., Giullitti, S., Forcato, M., Bicciato, S., Panzetta, V., Fusco, S., et al., 2020. Reprogramming normal cells into tumour precursors requires ECM stiffness and oncogene-mediated changes of cell mechanical properties. *Nat. Mater.* 19, 797–806.

- Park, J.Y., Yoo, S.J., Lee, E.J., Lee, D.H., Kim, J.Y., Lee, S.H., 2010. Increased poly(dimethylsiloxane) stiffness improves viability and morphology of mouse fibroblast cells. *Biochip J.* 4, 230–236.
- Paszek, M.J., Zahir, N., Johnson, K.R., Lakins, J.N., Rozenberg, G.I., Gefen, A., Reinhart-King, C.A., Margulies, S.S., Dembo, M., Boettiger, D., et al., 2005. Tensional homeostasis and the malignant phenotype. *Cancer Cell* 8, 241–254.
- Pijuan, J., Barceló, C., Moreno, D.F., Maiques, O., Sisó, P., Martí, R.M., Macià, A., Panosa, A., 2019. In vitro cell migration, invasion, and adhesion assays: from cell imaging to data analysis. *Front. Cell Dev. Biol.* 7, 107.
- Provenzano, P.P., Inman, D.R., Eliceiri, K.W., Knittel, J.G., Yan, L., Rueden, C.T., White, J.G., Keely, P.J., 2008. Collagen density promotes mammary tumor initiation and progression. *BMC Med.* 6, 11.
- Ritch, S.J., Brandhagen, B.N., Goyeneche, A.A., Telleria, C.M., 2019. Advanced assessment of migration and invasion of cancer cells in response to mifepristone therapy using double fluorescence cytochemical labeling. *BMC Cancer* 19, 376.
- Seghir, R., Arscott, S., 2015. Extended PDMS stiffness range for flexible systems. *Sensors Actuators A Phys.* 230, 33–39.
- Shreberk-Shaked, M., Oren, M., 2019. New insights into YAP/TAZ nucleo-cytoplasmic shuttling: new cancer therapeutic opportunities? *Mol. Oncol.* 13, 1335–1341.
- Sotiri, I., Tajik, A., Lai, Y., Zhang, C.T., Kovalenko, Y., Nemr, C.R., Ledoux, H., Alvarenga, J., Johnson, E., Patanwala, H.S., et al., 2018. Tunability of liquid-infused silicone materials for biointerfaces. *Biointerphases* 13, 06D401.
- Syed, S., Karadaghy, A., Zustiak, S., 2015. Simple polyacrylamide-based multiwell stiffness assay for the study of stiffness-dependent cell responses. *J. Vis. Exp.*
- Tahtamouni, L., Ahram, M., Koblinski, J., Rolfo, C., 2019. Molecular regulation of cancer cell migration, invasion, and metastasis. *Anal. Cell Pathol.*
- Ulbricht, A., Eppler, F.J., Tapia, V.E., Van Der Ven, P.F.M., Hampe, N., Hersch, N., Vakeel, P., Stadel, D., Haas, A., Saftig, P., et al., 2013. Cellular mechanotransduction relies on tension-induced and chaperone-assisted autophagy. *Curr. Biol.* 23, 430–435.
- Umesh, V., Rape, A.D., Ulrich, T.A., Kumar, S., 2014. Microenvironmental stiffness enhances glioma cell proliferation by stimulating epidermal growth factor receptor signaling. *PloS One* 9.
- Wu, L., Yang, X., 2018. Targeting the Hippo pathway for breast cancer therapy. *Cancers (Basel)* 10.
- Zanconato, F., Cordenonsi, M., Piccolo, S., 2016. YAP/TAZ at the roots of cancer. *Cancer Cell* 29, 783–803.